MOEM

Modern Electronic Materials 2023; 9(2): 77–90
DOI 10.3897/j.moem.9.2.109923

Review Article

Recent progress and development prospects of mobile current sources

Vladimir V. Sleptsov[1], Lev V. Kozhitov[2], Anna O. Diteleva[1], Dmitry Yu. Kukushkin[1], Alena V. Popkova[3]

1 Moscow Aviation Institute, 4 Volokolamskoe Highway, Moscow 125993, Russian Federation

2 National University of Science and Technology "MISIS", 4-1 Leninsky Ave., Moscow 119049, Russian Federation

3 JSC "Research Institute NPO" LUCH", 24 Zheleznodorozhnaya Str., Podolsk 142103, Russian Federation

Corresponding author: Anna O. Diteleva (anna.diteleva@mail.ru)

Received 11 May 2023 ♦ **Accepted** 3 June 2023 ♦ **Published** 6 July 2023

Citation: Sleptsov VV, Kozhitov LV, Diteleva AO, Kukushkin DYu, Popkova AV (2023) Recent progress and development prospects of mobile current sources. *Modern Electronic Materials* 9(2): 77–90. https://doi.org/10.3897/j.moem.9.2.109923

Abstract

Physicochemical fundamentals have been developed for the basic design solutions and fabrication technologies of prospective electrolytic power cells with a reusable cell capacity of 350–500 W·h/kg at the first stage and 1000 W·h/kg at the second stage. Along with conventional chemical current sources and ionistors, there are emerging high-performance supercapacitor structures with thin dielectric in the double electric layer and hybrid capacitors in which energy is accumulated in the double electric layer and due to electrochemical processes. This approach reduces the internal resistance of the electrolytic cells thus decreasing the heat emission during operation and therefore providing for a higher specific energy capacity and operation safety, shorter charging time and an increase in specific power. Prospective anode is a nanostructured electrode material in the form of a carbon matrix filled with a nanostructured chemically active material. Promising carbon matrix fillers are Li and its alloys, Si, Al, Na, Sn, Mg, Zn, Ni, Co, Ag, as well as a range of other materials and their compounds. The effect of carbon material specific surface area, dielectric permeability and chemically active material addition on the specific energy capacity has been studied. Theoretical specific energy capacity of metal/air hybrid capacitors has been calculated. Thin-film technological system has been designed for new generation electrode materials in the form of carbon matrices with highly developed surface containing thin tunneling dielectrics and chemically active materials on dielectric surface.

Keywords

hybrid capacitor, current sources, energy storage devices, carbon material, electrode materials, nanustructuring, nanoparticle, carbon matrix, chemically active material

1. Introduction

Sustained development of electrically driven vehicles, individual power supply systems for residential and industrial buildings, security systems and other applications requires, according to experts, reusable power sources with a specific energy capacity of 350–500 W·h/kg at the first stage and 1000 W·h/kg at the second stage. The highest capacity power sources manufactured by thick-film technologies are currently lithium chemical current sources **(LCS)** the highest energy capacity of which reaches 260 W·h/kg [1–3]. This technology is based on the synthesis of electrolytic cell electrodes by deposition of a 200–400 mm chemically active material layer on a metallic foil acting as a current collector [4–8]. Specific energy capacity growth has seen a stagnation over the re-

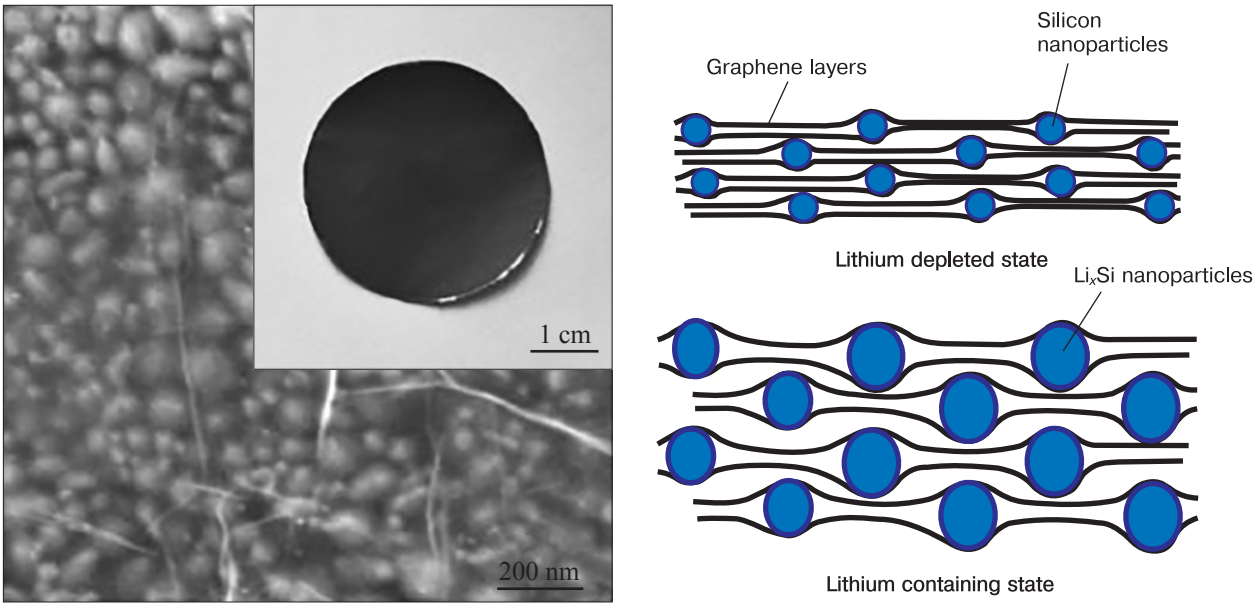

Figure 1. Appearance of high specific surface area carbon matrix anode with silicon nanoparticles

cent 10 years while the last year has demonstrated a trend of noticeably reducing the specific energy capacity aimed at ensuring higher device operation safety and lifetime. One can therefore assume that the existing thick film technologies have almost completely exhausted their energy capacity, operation safety and charging time reduction potential. Thus, achieving the above-listed specific energy capacity figures requires using new technologies, materials and designs to deliver a 2–4-fold specific energy capacity growth as compared with existing commercial chemical current sources **(CCS)** [9–12]. A prospective element base development roadmap [13] showed that the first stage will give a CCS performance growth in 2020–2025 at the expense of anode specific power growth. The anode structure will change fundamentally, to a carbon matrix with a high specific surface area (500–2000 m^2/g) filled with nanoparticles (Si, Ge, Sn, P and Sb) [1, 6–18]. Figure 1 shows example of a graphene-based elastic matrix with silicon nanoparticle filler used as a CCS anode, and Fig. 2 shows the energy capacity of that CCS anode as a function of number of cycles [1, 2, 17, 18].

Thus a promising CCS anode design is a nanostructured electrode material in the form of a carbon matrix filled with a nanostructured chemically active material. Since an elastic matrix has a high specific surface area, energy accumulation in the electrode material occurs by two mechanisms (due to electrochemical reactions and in the double electric layer **(DEL)**). As a result the electrochemical cell for 3–5-generation current sources is conceived to be a hybrid capacitor. Further CCS specific energy capacity growth to 500 W·h/kg and higher is associated, according to the roadmap, with the development of metal/sulfur and metal/air CCS in which the anode is connected to the cathode delivering sulfur or oxygen, respectively. The electrode materials for the CCS will be high specific surface area carbon matrices filled with functional materials in the form of chemically

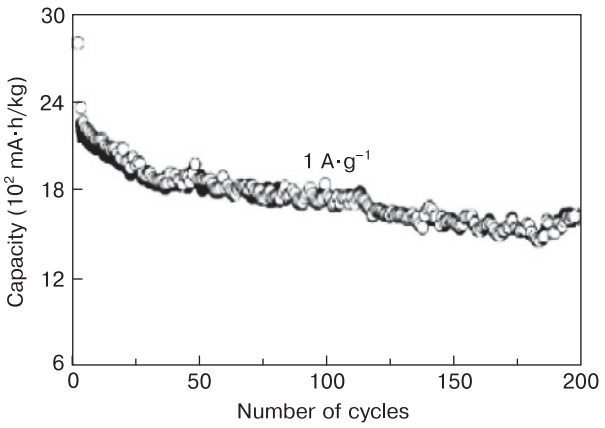

Figure 2. Energy capacity of high specific surface area carbon matrix CCS with silicon nanoparticles as a function of number of cycles

active and auxiliary materials. Promising carbon matrix filler materials are Li and its alloys, Si, Al, Na, Sn, Mg, Zn, Ni, Co, Ag and a number of other materials and their compounds [19–28]. The emergence of a new electrolytic materials generation entails a dramatic increase in the number of electrochemical power cell design options. Along with conventional CCS and ionistors, there are emerging high-performance supercapacitor structures (HPSS) with thin dielectric in the double electric layer and hybrid capacitors in which energy is accumulated in the DEL and due to electrochemical processes. This approach reduces the internal resistance of the electrolytic cells thus decreasing the heat emission during operation and therefore providing greater specific energy capacity and operation safety, shorter charging time and specific power output growth.

Since the research into current sources implementing DEL and electrochemical process based energy accumulation mechanisms has led to the development of multiple

electrochemical cell design options (CCS, ionistors, high-performance supercapacitors with thin tunneling dielectric in DEL and hybrid capacitors), there is the necessity to develop physical and mathematical models describing the basic design, material science and technical solutions of the prospective element base.

2. Theoretical analysis of prospective electrolytic cell designs

Theoretical analysis of energy accumulation in electrode materials of hybrid capacitors based on a thermodynamical approach implying the summation of all energy types in the system in question allows writing the energy balance equation for the hybrid capacitor as follows:

$$\frac{CU_c^2}{2} + \sum M_i N_i = I_L U_L t + I_c^2 R_{ESR} t, \quad (1)$$

where C is the capacity, U_c is the capacitor voltage, M_iN_i is the product of chemical potential and the number of particles, I_L is the load current, U_L is the load voltage, t is the charging/discharging time, I_c is the capacitor current and R_{ESR} is the electrical resistance of the capacitor structure.

Equation (1) describes the ideal capacitor free of leakage currents. To simplify the problem one can consider the operation of that capacitor for minimum charging/discharging time. Simple transformations of Eq. (1) yield the following equation of the capacitor energy E_c:

$$E_c = \left(\frac{\varepsilon \varepsilon_0}{2d} U_c^2 + iU_c t - I_c^2 \frac{R_{ESR}}{S^2} t \right) S, \quad (2)$$

where ε is the dielectric permeability, ε_0 is the relative dielectric permeability, i is the electrochemical reaction rate, U_c is the capacitor voltage, t is the charging/discharging time, I_c is the capacitor current, R_{ESR} is the electrical resistance of the capacitor structure, S is the surface area and d is the double electric layer thickness.

The electrochemical reaction rate (in A/cm^2 or A/m^2) is commonly related to a specific surface area and defined as current density:

$$i = \frac{I}{S}.$$

It can be seen that the specific energy capacity of a hybrid capacitor is determined by the sum of the interrelated parameters R_{ESR}, S, U_c, I_c and t.

Equation (2) describes the ideal hybrid capacitor free of leakage currents. To simplify the task one can consider the operation of that capacitor for minimum charging/discharging time.

FractalCalculation software was designed for capacitor parameter calculation in Python programming language, code UTF-8. Python is one of the most widely used cross-platform programming languages. FractalCalculation incorporates two blocks with software code describing software operation principle: 1) data calculation, acquisition and displaying algorithm and 2) UI (user interface) software code or, simply, what the user works with.

Based on the mathematical model developed, the specific energy capacity of prospective electrolytic cell designs was calculated: 1) ionistors, i.e., high-performance supercapacitors the specific energy capacity of which is determined, primarily, by the specific surface area of the electrode materials; 2) high-performance supercapacitors with thin tunneling dielectric in the double electric layer, the dielectric permeability of which can be varied over a wide range; 3) hybrid capacitors in which energy is accumulated in the DEL and due to chemical reactions; 4) hybrid capacitors with thin tunneling dielectric in the DEL, the dielectric permeability of which can be varied over a wide range and energy is accumulated in the DEL and due to chemical reactions.

2.1. Ionistors: high-performance supercapacitors

The specific energy capacity of ionistors is determined, primarily, by the specific surface area of the electrode materials. The effect of the specific surface area of the electrode material (300–3000 m^2/g) on the specific energy capacity of cells was studied for a constant dielectric permeability using the energy balance equation and the software designed. The unknown parameter for the calculation was the thickness d for water and polymer electrolyte cells. Table 1 summarizes the parameters of the model water and polymer electrolyte capacitors fabricated in which the cell electrode material was Busofit type porous carbon material with a 1200 m^2/g specific surface area. The electrical parameters of the cells were measured on a ESK-2.21 cyclic test bed [29, 30].

The specific energy capacity of the cells (E_{sp}, W·h/kg) was calculated using the formula

$$E_{sp} = \frac{E}{3600\,m} = \frac{\left(\frac{\varepsilon \varepsilon_0}{2d} U_c^2 + iU_c t - I_c^2 \frac{R_{ESR}}{S^2} t \right) S}{3600\,m}, \quad (3)$$

where m is the cell weight.

Since the calculation is conducted for capacitors, $iU_ct = 0$ and Eq. (3) can be rewritten as follows:

$$E_{sp} = \frac{E}{3600\,m} = \frac{\left(\frac{\varepsilon \varepsilon_0}{2d} U_c^2 - I_c^2 \frac{R_{ESR}}{S^2} t \right) S}{3600\,m}. \quad (4)$$

The thickness of the DEL calculated using Eq. (4) was $d_{av.wat} \sim 13.8$ for water electrolyte specimens and $d_{av.polym} \sim 1.0$ for polymer electrolyte specimens.

Based on the calculated and experimental data (Table 1) we studied the effect of an increase in the specific surface area of the electrode material from 300 to 3000 m^2/g on the specific energy capacity of the cells (Fig. 3).

Table 1. Parameters of water and polymer electrolyte cells

Cell #	Busofit fabric area (cm^2)	Weight of Busofit fabric with preset dimensions (g)	Outer surface area (m^2)	Charging / discharging voltage (V)	Charging / discharging current (A)	Time (s)	Capacity (F)	Energy capacity (W·h/kg)	ESR (Ohm)	Weight (g)	Software-calculated parameters	
											d (nm)	*i*
Water electrolyte cells (dielectric permeability $\varepsilon_{wat} \sim 80$)												
1	60	1.43	1716	2.5	0.15	865	87	4.2	1.47	18	13.95	0
2	81	1.93	2316	2.5	0.15	2000	141	4.9	0.315	25	11.61	0
3	400	9.66	11592	2.5	0.15	6496	521	4.5	0.457	100	15.83	0
Polymer electrolyte cells (dielectric permeability $\varepsilon_{polym} \sim 8$)												
1	75	1.8	2160	4	0.5	460	151	16	1.0	20	1.1	0
2	192	4.61	5532	4.5	0.5	1200	355	21	1.5	46	0.9	0
3	340	8.1	9720	3.5	0.5	2400	570	12	0.3	80	0.6	0

The obtained curves allow determining the maximum theoretical energy capacity of the cell. The results suggest that no breakthrough in energy capacity growth was made.

2.2. High-performance supercapacitors with thin-tunneling dielectric in DEL

The dielectric permeability of this type of capacitors varies over a wide range. Such material can be for example potassium polytitanate **(PPT)**. At a TiO_2/K_2O molar ratio of 3.7 to 6.6 this material is in the form of layered scale-shaped particles 200–800 nm in width and 10–40 in thickness. The electrical conductivity and dielectric permeability of PPT may exhibit figures typical of solid state electrolytes, semiconductors or dielectrics. The dielectric permeability of PPT may vary from 10^3 to 10^9 (Fig. 4) [31, 32].

The effect of an increase in the dielectric permeability ($\varepsilon \sim 5 \cdot 10^5$) due to the formation of a 10–20 nm thin-tunneling dielectric layer was studied.

The calculations were made for cells with an electrode material specific surface area of 1200 m^2/g. Figure 5 shows the specific energy capacity of water and polymer electrolyte cells as a function of dielectric permeability for different specimens at 4.5 V.

Study of the effect of an increase in the dielectric permeability (up to 10^5) due to the formation of a 10–20 nm thin-tunneling dielectric layer showed that the maximum theoretical specific energy capacity can reach 9 kW·h/kg for water electrolyte capacitors and 30 kW·h/kg for polymer electrolyte capacitors. These results are quite approximate since the mathematical model still has a space for improvement by taking into account the effect of electrolyte and working voltage, potentially providing for a significant breakthrough in energy capacity. One should also bear in mind that the presence of a thin dielectric layer in the DEL may increase the working voltage to far above the CCS-typical figures. For example, the working voltage of aluminum capacitors may grow to 1000 V and that of tantalum ones, to 70 V.

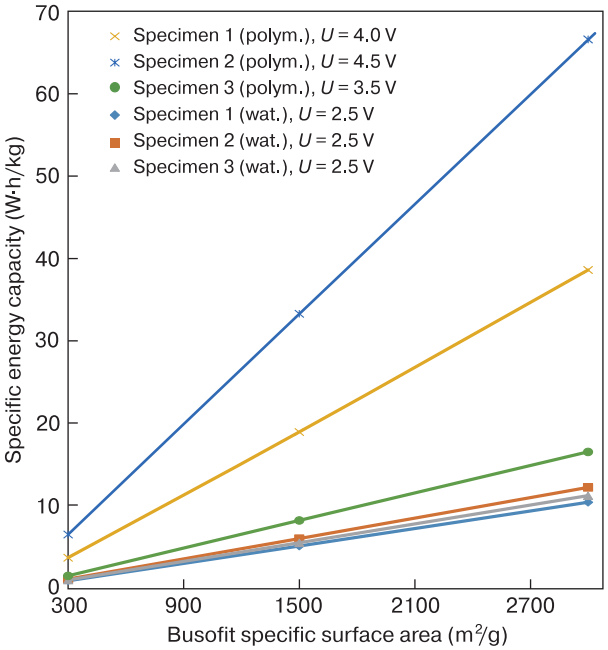

Figure 3. Specific energy capacity of water and polymer electrolyte cells as a function of Busofit specific surface area

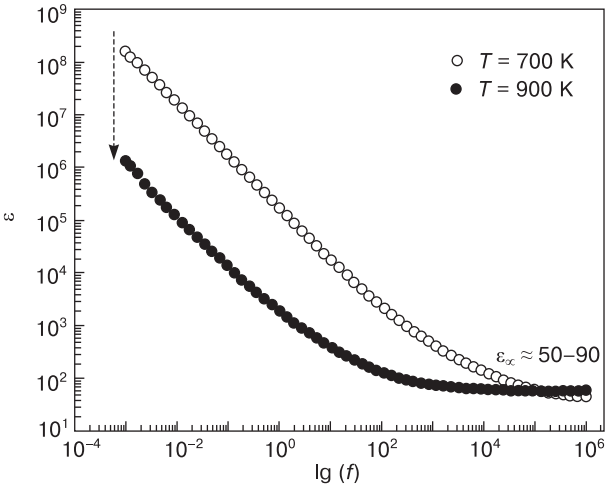

Figure 4. Fe-modified potassium polytitanate

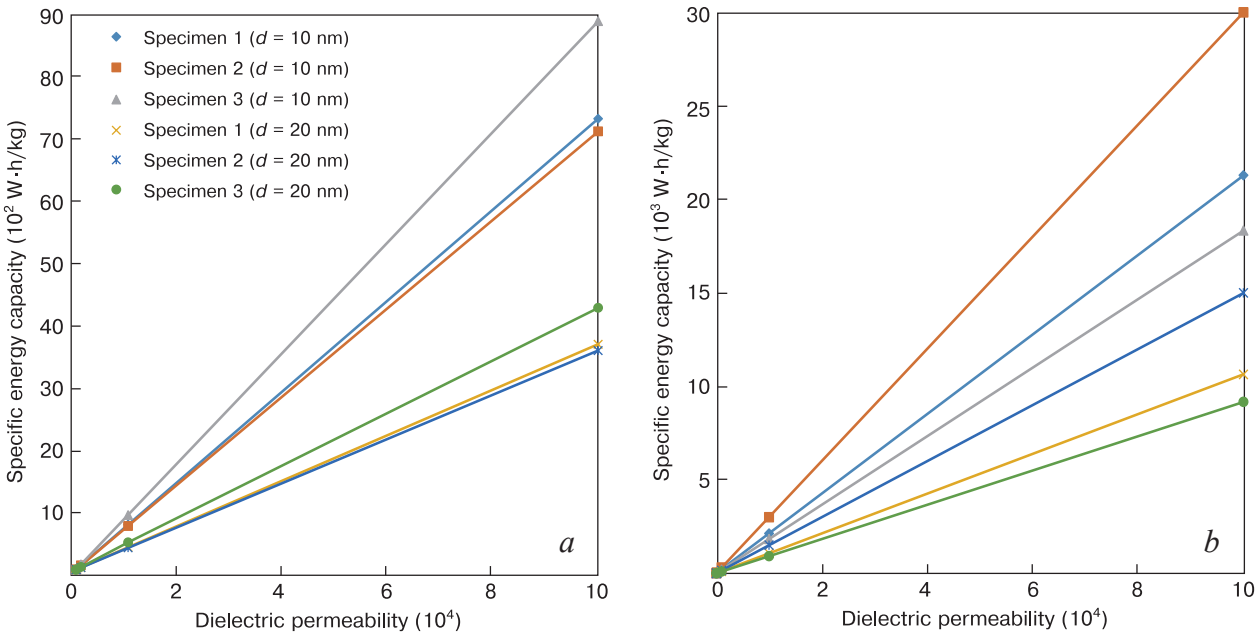

Figure 5. Specific energy capacity of (*a*) water and (*b*) polymer electrolyte cells as a function of dielectric permeability for different thin-tunneling dielectric thickness

2.3. Hybrid capacitors

Energy is accumulated in hybrid capacitors in the DEL and due to chemical reactions. For energy capacity calculations, $LiNi_{0.8}Co_{0.15}Al_{0.05}O_2$ additive deposited onto the cathode material of capacitors was used as a chemically active material **(CAM)** (Specimens 1, 2 and 3) and the parameters of that cathode material are summarized in Table 2.

The energy capacity E_{CCS} is 760 W·h/kg for $LiNi_{0.8}Co_{0.15}Al_{0.05}O_2$ battery cathode and 500 W·h/kg for water electrolyte cells at 2.5 V. This allows calculating the energy capacity delivered by the CAM additive m_{CAM} which is k percents of the hybrid capacitor weight.

$$E_{m.CCS} = E_{CCS}m_{CAM},$$

where $m_{CAM} = km_{hybr}$.

The specific capacitor energy capacity $E_{m.cap}$ per its weight m can be calculated using the following formula:

$$E_{m.cap} = E_{sp}m.$$

The specific energy capacities E_{sp} of capacitors having the weight m are summarized in Table 1.

Since the weight of the cathode material is 50% of the cell weight, the hybrid specimen weight m_{hybr} can be calculated using the following formula:

$$m_{hybr} = m + m_{CCS} = m + 0.5m.$$

The specific energy capacity of a hybrid capacitor with CAM is calculated as follows:

$$E_{hybr} = \frac{E_{m.cap} + E_{m.CCS}}{m_{hybr}}. \quad (5)$$

Table 2. Specific energy capacities of hybrid capacitors with CAM additions

Specimen No.	Capacitor weight (g)	Specific energy capacity without CAM E_{sp} (W·h/kg)	Hybrid capacitor specific energy capacity at E_{hybr} (W·h/kg)			
			CAM weight 5 % of hybrid capacitor weight	CAM weight 15 % of hybrid capacitor weight	CAM weight 35 % of hybrid capacitor weight	CAM weight 50 % of hybrid capacitor weight
Water electrolyte cells ($\varepsilon_{wat} \sim 80$, $d_{av.wat} \sim 13.8$ nm)						
1	18	4.2	28	78	178	253
2	25	4.9	28	78	178	253
3	100	4.5	28	78	178	253
Polymer electrolyte cells ($\varepsilon_{polym} \sim 8$, $d_{av.polym} \sim 1.0$ nm)						
1	20	16	49	125	276	390
2	46	21	52	128	280	394
3	80	12	46	122	274	388

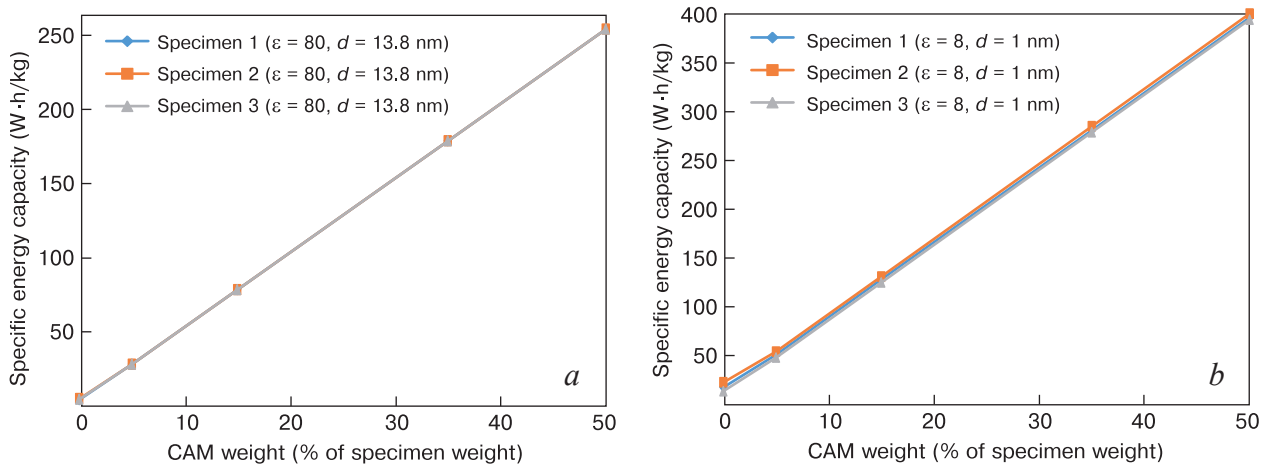

Figure 6. Specific energy capacity of (*a*) water and (*b*) polymer electrolyte hybrid capacitors as a function of CAM content

Table 2 shows calculated specific energy capacities of hybrid capacitors with a 5–50% CAM percentage of cell weight. Figure 6 shows specific energy capacities of water and polymer electrolyte hybrid capacitors with CAM additions of 0 to 50% of cell weight.

The calculations suggest that the energy capacity of electrochemical cells can grow to max. 350–400 W·h/kg. Further growth of the specific energy capacity requires transition to lithium/air CCS cell design and new technologies and materials. It should be noted that in that case, thin-film technologies are also helpful for solving the task.

2.4. Hybrid capacitosr with thin-tunneling dielectric in DEL

The dielectric permeability of this type of capacitors varies over a wide range, the energy being accumulated in the DEL and due to chemical reactions. Specific energy capacities were calculated for hybrid capacitors with thin-tunneling dielectric in the DEL and a dielectric permeability of 10^3 for water electrolyte cells and 10^2 for polymer electrolyte cells (Table 3, Fig. 7). $LiNi_{0.8}Co_{0.15}Al_{0.05}O_2$ was used as CAM.

If conventional cathode materials are used, no appreciable growth in specific energy capacity can be achieved even with new anodes (see Fig. 2) the weight of which is 5–10% greater due to the respective reduction of anode weight.

However, the result can be improved by using new electrolytic cell designs e.g. air/lithium CCS. The development of those electrolytic cells requires new technologies. One option is to use thin-film technologies.

Specific energy capacities of hybrid capacitors were calculated for ZnO and LiO_2 metal/air systems (Tables 4 and 5) and their charts were plotted (Figs. 8 and 9). The energy capacity of ZnO/air CCS proved to be 902 W·h/kg and that of LiO_2/air CCS, 10811 W·h/kg for polymer electrolyte (Table 5) and 9130 W·h/kg for water electrolyte at 2.5 V.

The calculations suggest that even if a thin-tunneling dielectric with a relatively low dielectric permeability is used, conventional chemically active materials allow achieving CCS with a specific energy capacity

Table 3. Specific energy capacities for hybrid capacitors with high dielectric permeability and CAM additions

Specimen No.	Capacitor weight (g)	Specific energy capacity without CAM E_{sp} (W·h/kg)	Hybrid capacitor specific energy capacity at E_{hybr} (W·h/kg)			
			CAM weight 5 % of hybrid capacitor weight	CAM weight 15 % of hybrid capacitor weight	CAM weight 35 % of hybrid capacitor weight	CAM weight 50 % of hybrid capacitor weight
Water electrolyte cells ($\varepsilon_{wat} \sim 10^3$, $d_{av.wat} \sim 13.8$ nm)						
1	18	53	60	110	210	285
2	25	52	60	110	210	285
3	100	65	68	118	218	293
Polymer electrolyte cells ($\varepsilon_{polym} \sim 10^2$, $d_{av.polym} \sim 1.0$ nm)						
1	20	212	179	255	407	521
2	46	299	237	313	465	579
3	80	182	159	235	287	501

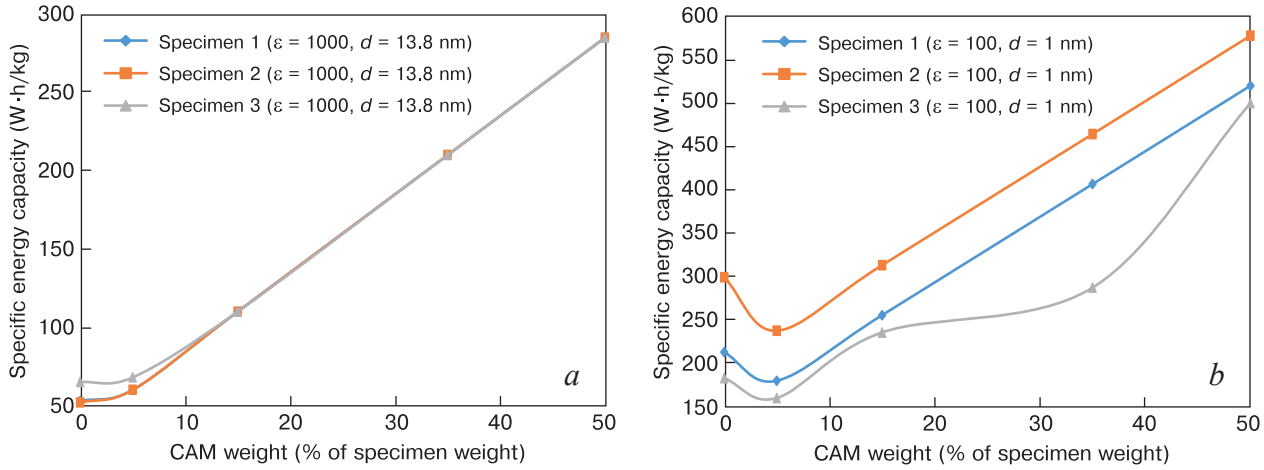

Figure 7. Specific energy capacity of (*a*) water and (*b*) polymer electrolyte high dielectric permeability hybrid capacitors as a function of CAM content

Table 4. Specific energy capacities of hybrid capacitors with ZnO metal/air system

Specimen No.	Capacitor weight (g)	Specific energy capacity without CAM E_{sp} (W·h/kg)	Hybrid capacitor specific energy capacity at E_{hybr} (W·h/kg)			
			CAM weight 5 % of hybrid capacitor weight	CAM weight 15 % of hybrid capacitor weight	CAM weight 35 % of hybrid capacitor weight	CAM weight 50 % of hybrid capacitor weight
Water electrolyte cells ($\varepsilon_{wat} \sim 10^3$, $d_{av.wat} \sim 13.8$ nm)						
1	18	53	80	170	351	486
2	25	52	80	170	351	486
3	100	65	88	179	359	494
Polymer electrolyte cells ($\varepsilon_{polym} \sim 10^2$, $d_{av.polym} \sim 1.0$ nm)						
1	20	212	186	276	457	592
2	46	299	244	334	515	650
3	80	182	166	256	437	572

of 400–500 W·h/kg, and the specific energy capacity will grow dramatically if the lithium/air system is used.

Theoretical analysis of prospective electrolytic cells suggests the necessity of developing a thin-film technology providing for the fabrication of new generation electrode materials designed in the form of a carbon matrix with a well-developed surface containing a thin-tunneling dielectric with CAM on its surface. The main task of this technology is to provide for the deposition of nanostructured functional layers on the carbon matrix

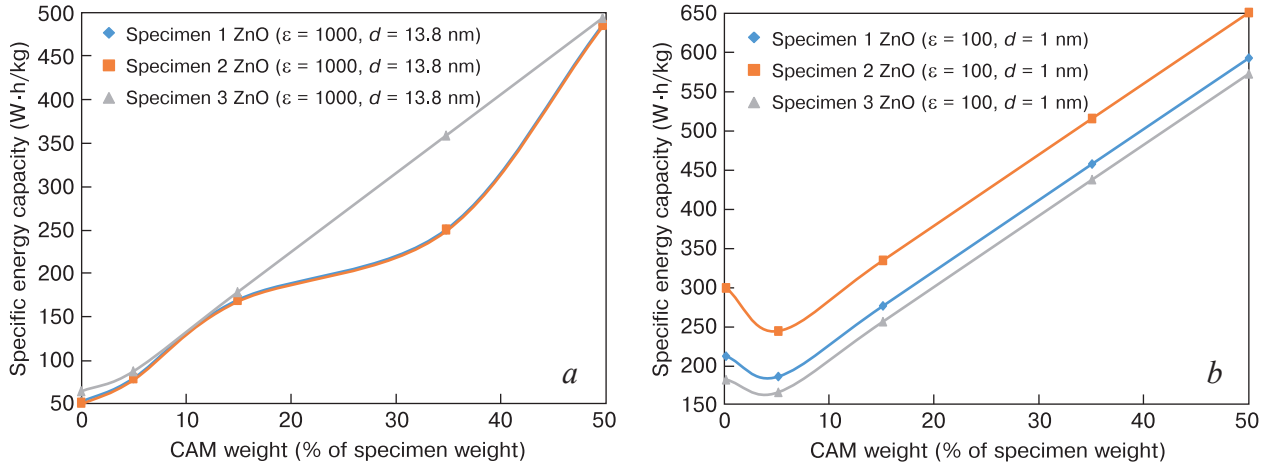

Figure 8. Specific energy capacity of (*a*) water and (*b*) polymer electrolyte hybrid capacitors with ZnO metal/air system as a function of CAM content

Table 5. Specific energy capacities of hybrid capacitors with LiO_2 metal/air system

Specimen No.	Capacitor weight (g)	Specific energy capacity without CAM E_{sp} (W·h/kg)	Hybrid capacitor specific energy capacity at E_{hybr} (W·h/kg)			
			CAM weight 5 % of hybrid capacitor weight	CAM weight 15 % of hybrid capacitor weight	CAM weight 35 % of hybrid capacitor weight	CAM weight 50 % of hybrid capacitor weight
Water electrolyte cells ($\varepsilon_{wat} \sim 10^3$, $d_{av.wat} \sim 13.8$ nm)						
1	18	53	492	1404	3230	4600
2	25	52	492	1404	3230	4600
3	100	65	500	1413	3239	4608
Polymer electrolyte cells ($\varepsilon_{polym} \sim 10^2$, $d_{av.polym} \sim 1.0$ nm)						
1	20	212	682	1763	3925	5547
2	46	299	740	1821	3983	5605
3	80	182	662	1743	3905	5527

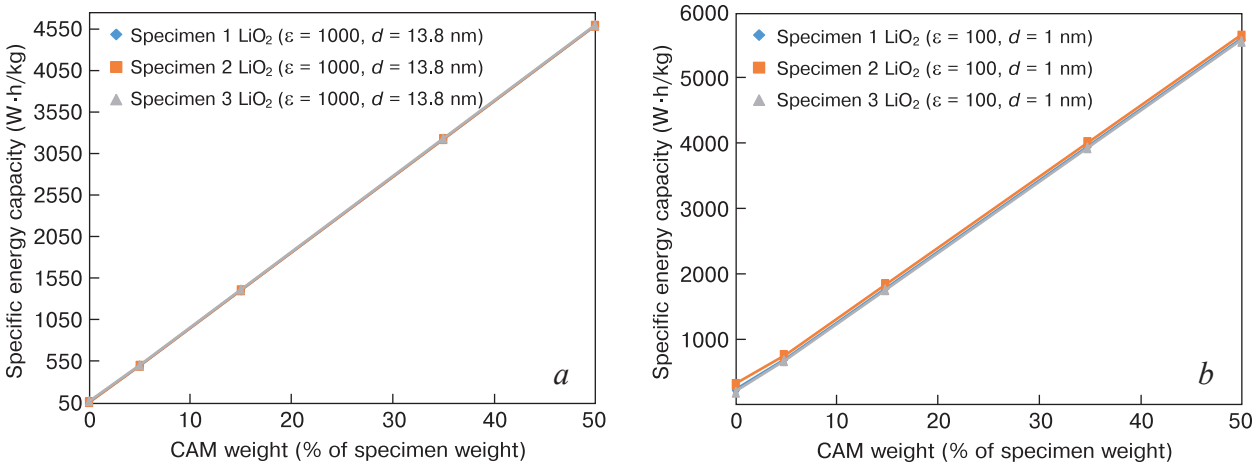

Figure 9. Specific energy capacity of (*a*) water and (*b*) polymer electrolyte hybrid capacitors with LiO_2 metal/air system as a function of CAM content

with a high specific surface area (450–500 m^2/g or higher). Theoretical analysis suggests that high specific energy capacities can be achieved by providing a hybrid capacitor with a thin tunneling dielectric in the DEL and CCS in which lithium or its alloys are used as CAM. Solution of this task requires a technological system providing for the fabrication of high specific surface area matrices containing a thin-tunneling dielectric to accommodate CAM. Thin-film technologies are a promising development trend and therefore theoretical and physicochemical fundamentals of these technologies are being developed.

3. Technological system development

3.1. Development and testing of elastic carbon matrix for electrode materials of capacitor structures

This work deals with a thin-film technology of CCS, high-performance supercapacitor systems and hybrid high-performance supercapacitor systems on the basis of a unified electrode material, which is justified by the physical and mathematical model being developed.

Study of the thin-film technology for active layer deposition on highly developed surface carbon matrices allows reducing the internal resistance of the electrolytic cells by orders of magnitude. Since the heat emission due to current passage in the system is described by the formula

$$Q = I^2R,$$

the temperature decreases dramatically and hence the operation safety of the electrolytic cells increases.

Thus, a promising electrode material for hybrid capacitor structures is a nanostructured electrode material in the form of a carbon based matrix filled with nanostructured CAM.

Since an elastic matrix has a high specific surface area, energy accumulation in the electrode material occurs by two mechanisms: due to chemical reactions and in the DEL.

Figure 10. UMRM-1 vacuum plant

Carbon matrix metallization includes two stages:

First stage: magnetron vacuum titanium layer deposition on a UMRM-1 roll stand type system [30, 33].

Titanium was chosen due to its low weight and the possibility of eventually synthesizing sodium and potassium polytitanate. Appropriate processing of this material allows synthesizing high dielectric permeability coatings (above 10^6).

Second stage: coating of deeper layers and formation of target nanostructure by electropulse technologies.

The UMRM-1 technological system (Fig. 10) is designed for the metallization of carbon materials e.g. Busofit T-40 synthesized in the form of fabric for electrolytic cells.

The equipment was designed for operation in moderate and cold climate, location category 4 as per GOST 15150-69[1] for locations with a (22 ± 3)°C air temperature and a (60 ± 15)% relative humidity.

The equipment is powered from three-phase four-wire mains with a neutral wire, 380/220 V, 50 Hz, power supply quality standard as per GOST 13109-87[2].

The equipment operation principle is titanium magnetron vacuum sputtering and titanium vapor condensation on a Busofit T-40 type carbon material a tape of which is run on the winding tolls over three evaporation zones [30].

Figure 11 *a* shows a photograph of source Busofit T-40 type carbon material surface without coating, and

[1] Interstate standard. Machines, devices and other technical products. (In Russ.). https://docs.cntd.ru/document/1200003320

[2] Interstate standard. Electric energy. Electromagnetic compatibility of technical equipment. Power quality limits in public electrical systems. (In Russ.). https://docs.cntd.ru/document/1200006034

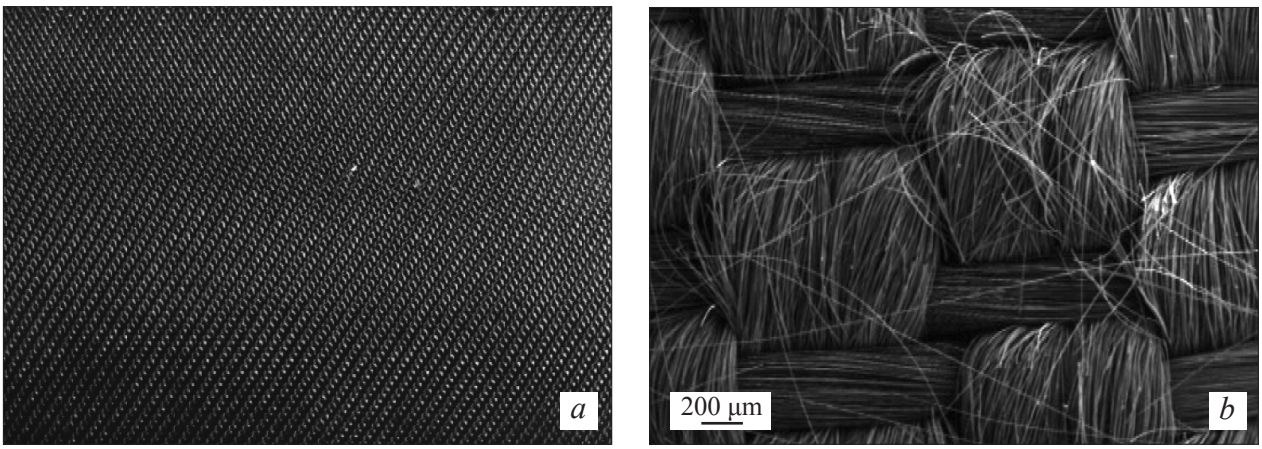

Figure 11. Photographs of (*a*) uncoated and (*b*) coated Busofit type fabric

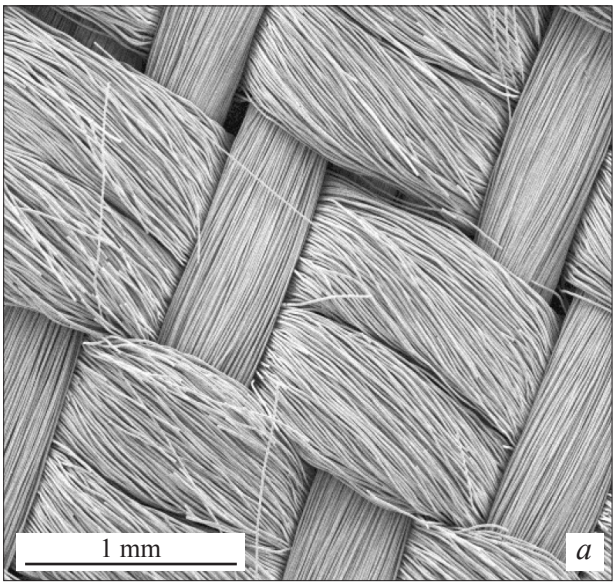

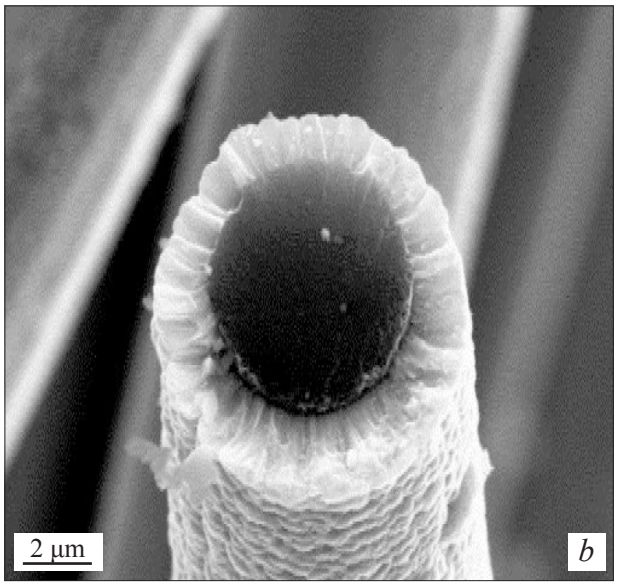

Figure 12. Photograph of Busofit type fabric with titanium layer applied: (*a*) high-magnification photograph; (*b*) electron micrograph. Thread thickness 6.131 mm, metal layer thickness 2.052 mm

Fig. 12 shows photographs and electron micrographs of Busofit T-40 type material with a metal layer coating on the surface. The metal layer also acts as a current collector [30].

Figure 12 also shows a discrete thread of Busofit type fabric with a titanium layer applied.

The metal layer on Busofit type fabric reduces the internal resistance and increases the capacity of the electrolytic cell. A more complex technical task of applying a metal layer on each thread is solved by integration of a vacuum metallization technology with an electropulse technology of nanoparticle formation in liquid media. The surface to be coated is covered with a film having a pillar structure with a highly developed surface.

Figure 13. Electrode unit of electropulse plant for nanoparticle formation in liquid media

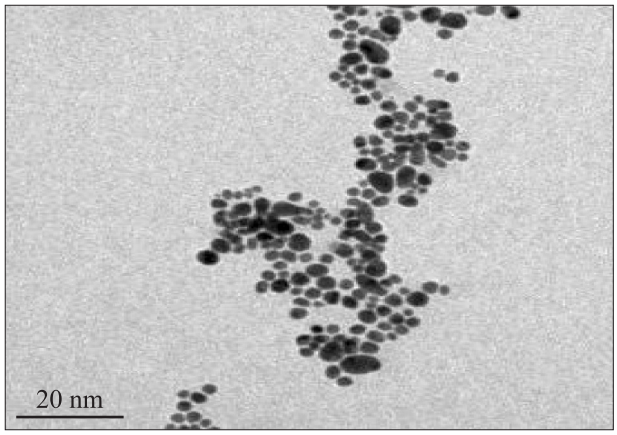

Figure 14. Silver nanoparticle in distilled water

To date, the minimum experimental Busofit type fabric thickness is 250–300 mm which is 45–50 thread layers stacked one upon another. It is therefore impossible to apply metallization layers on each thread (over the whole fabric depth) in vacuum. Then a liquid phase nanoparticle deposition technology is used. Figure 13 shows the basic equipment module for liquid phase nanoparticle deposition and Fig. 14 shows a silver nanoparticle in distilled water.

This task was solved by developing a liquid phase coating deposition technology for which the target fabric is completely submerged in a metal nanoparticle-containing liquid for particle penetration to each individual thread.

Figure 15 shows electron micrographs of silver nanoparticle-metalized Busofit type fabric fibers.

One can see silver aggregation on the surface in the form of large nanoparticles and crystals which develop

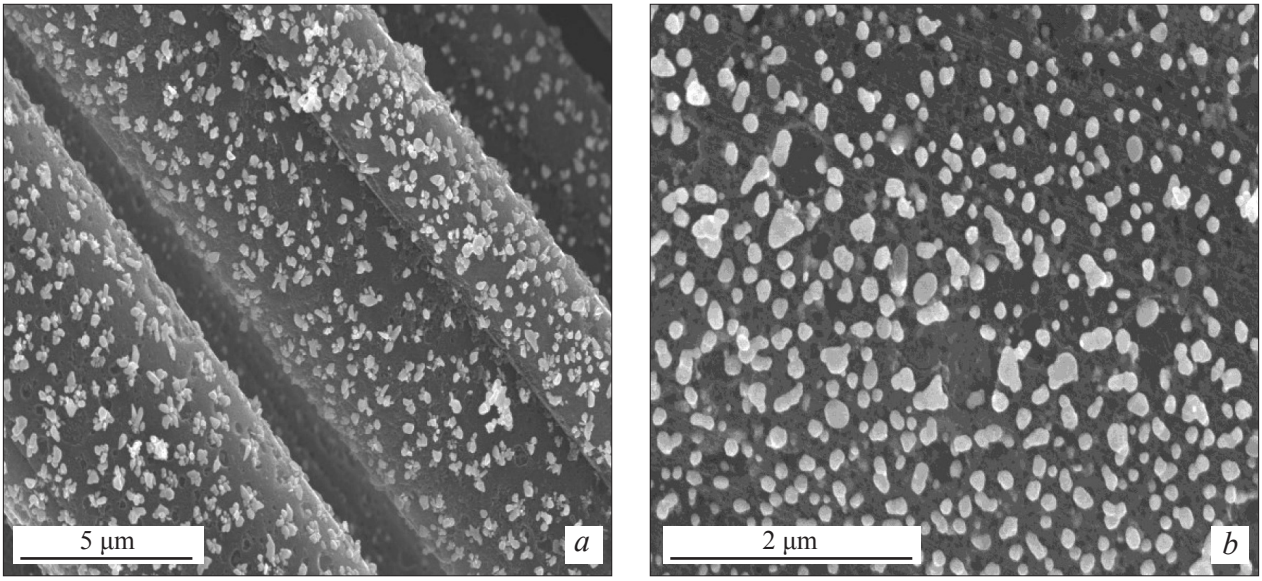

Figure 15. Complex metallization of Busofit type fabric: (*a*) vacuum titanium application and (*b*) silver and nickel application

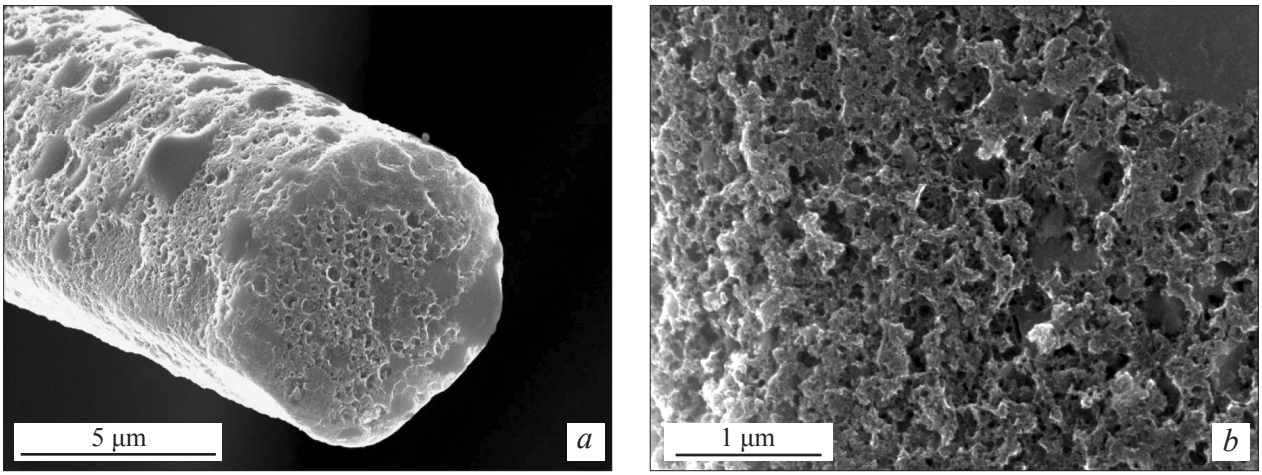

Figure 16. Carbon matrix thread with nanostructured aluminum layer

the fiber surface. Figure 16 shows a Busofit type fabric thread covered with an aluminum layer formed from nanoparticles.

Zinc and magnesium layers were also deposited on the carbon matrix during tests (Fig. 17).

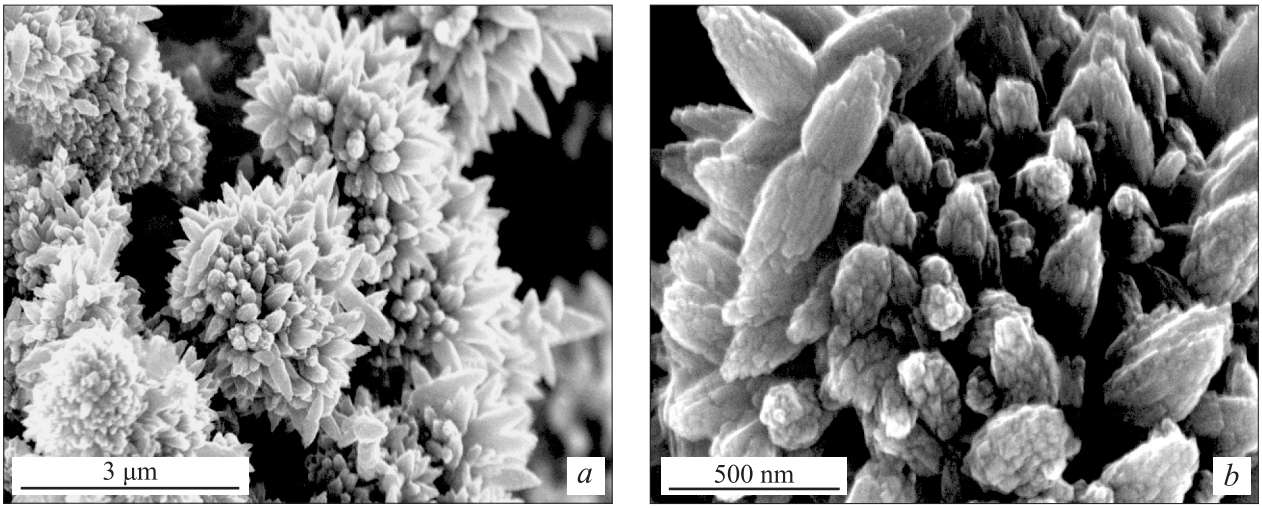

Figure 17. Carbon matrix thread with nanostructured zinc layer

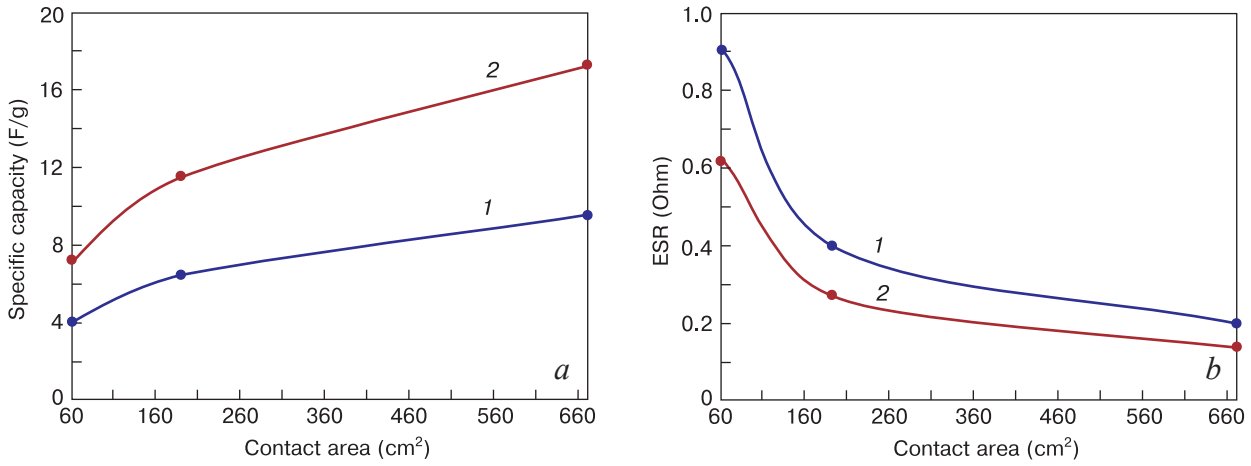

Figure 18. (*a*) Specific electrical capacity and (*b*) electrical resistance of ESR capacitor structure as a function of electrode material contact area in cells: (*1*) without metallization and (*2*) with metallization

The electrode materials obtained were used for synthesizing high-performance supercapacitors and DEL the appearance of which is shown in Fig. 16. Capacity proves to depend, primarily, on the electrode material surface area (Fig. 18, Curve *1*) [29, 30]. Metal layer deposition on Busofit type fabric reduces the internal resistance and increases the specific energy capacity of electrolytic cells.

It is safe to assume that a decrease in the electrical resistance of the capacitor structure increases its specific energy capacity, and that thin-film technologies, unlike conventional thick-film ones, allow controlling this parameter over a wide range. The assembled capacitor structures were bed-tested for residual water removal aiming at achieving a higher operation voltage. The operation voltage could be increased to 4.5–5 V, corresponding to a maximum specific energy capacity of 25–30 Q·h/kg. Theoretically, the structure in question can be operated at voltages of above 5 V for dry-room assembly, i.e., in the complete absence of moisture. Then the specific energy capacity of cells can exceed the capacity of lead batteries.

Cyclic tests of bed specimens (Fig. 19) with 50 or more cycles showed stable operation at 0 to 4000 mV. No electrolyte decomposition traces were observed in this voltage range. Similar results were obtained for 0 to 6000 mV (see Fig. 19) indicating the absence of electrochemical modification in the electrolyte or oxidation/reduction reactions at electrodes [31–33].

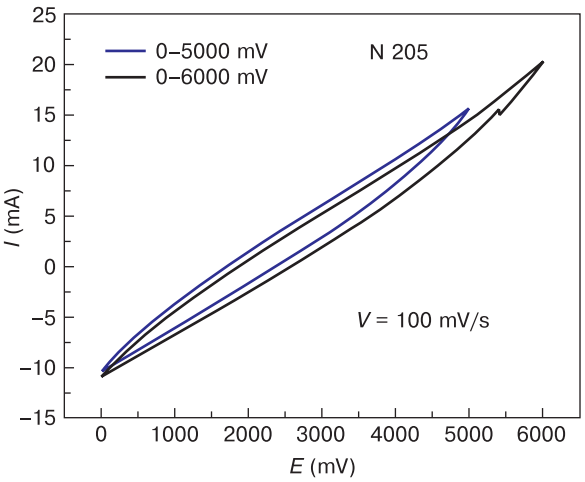

Figure 19. Cyclie C–V chart (bias rate 10 mV/s) for symmetrical energy storage with titanium-modified electrodes

4. Conclusion

Prospective electrolytic energy storage cell designs were studied. We show that a significant increase in the specific energy capacity can be achieved in capacitors with thin-tunneling dielectric in the double electric layer and in hybrid capacitors with the DEL containing a thin-tunneling dielectric layer.

A thin-film technological system was developed for the synthesis of nanostructured materials on carbon matrices with different specific surface areas allowing the manufacture of electrolytic cells and ensuring their specific energy capacity growth.

Acknowledgements

This work was carried out within State Assignment of the Ministry of Education and Science of the Russian Federation, Topic No. FSFF-2023-0008.

References

1. Skleznev A.A. Analysis of the main trends in the development of chemical current sources and other energy storage devices. Moscow; 2017. (In Russ.)
2. Sleptsov V.V., Zinin Yu.V., Diteleva A.O. Future development of the mobile energy. *Uspekhi v khimii i khimicheskoi tekhnologii*. 2019; 33(1(211)): 28–30. (In Russ.)
3. Zhang X., Qu N., Yang S., Lei D., Liu A., Zhou Q. Cobalt induced growth of hollow MOF spheres for high performance super-capacitors. *Materials Chemistry Frontiers*. 2021; (5): 482–491. https://doi.org/10.1039/D0QM00597E
4. Liu X., Shi C., Zhai C., Cheng M., Liu Q., Wang G. Cobalt-based layered metal-organic framework as an ultrahigh capacity supercapacitor electrode material. *ACS Applied Materials and Interfaces*. 2016; 8(7): 4585–4591. https://doi.org/10.1021/acsami.5b10781
5. Yang J., Ma Z., Gao W., Wei M. Layered structural co-based MOF with conductive network frames as a new super-capacitor electrode. *Chemistry-A European Journal*. 2017; 23(3): 631–636. https://doi.org/10.1002/chem.201604071
6. Zhang Y., Wang Y., Xie Y.-L., Cheng T., Lai W., Pang H., Huang W. Porous hollow Co_3O_4 with rhombic dodecahedral structures for high-performance super-capacitors. *Nanoscale*. 2014; 6(23): 14354–14359. https://doi.org/10.1039/c4nr04782f
7. Mukhiya T., Ojha G.P., Dahal B., Kim T., Chhetri K., Lee M., Chae S.-H., Muthurasu A., Tiwari A.P., Kim H.Y. Designed assembly of porous cobalt oxide/carbon nanotentacles on electrospun hol-low carbon nanofibers network for supercapacitor. *ACS Applied Energy Materials*. 2020; 3: 3435–3444. https://doi.org/10.1021/acsaem.9b02501
8. Lebedeva N., Di Persio F., Boon- Brett L. Lithium-ion battery value chain and related opportunities for Europe. EUR 28534 EN, Publications Office of the European Union, Luxembourg; 2017: JRC105010. 25 p. https://doi.org/10.2760/6060
9. Lebedev E.A. Development of formation processes and research of properties of elements of heat generation and energy storage for thermoelectric batteries. Diss. Cand. Sci. (Eng.). Moscow; 2017. 184 p. (In Russ.)
10. Hou S., Lian Y., Bai Y., Zhou Q., Ban Ch., Wang Zh., Zhao J., Zhang H. Hollow dodecahedral Co_3S_4@NiO derived from ZIF-67 for supercapacitor. *Electrochimica Acta*. 2020; 341: 136053. https://doi.org/10.1016/j.electacta.2020.136053
11. Bai X., Liu J., Liu Q., Chen R., Jing X., Li B., Wang J. In-situ fabrication of MOF-derived co-co layered double hydroxide hollow Nanocages/Graphene composite: a novel electrode material with superior electrochemical performance. *Chemistry-A European Journal*. 2017; 23(59): 14839–14847. https://doi.org/10.1002/chem.201702676
12. Kim T., Song W., Son D.-Y., Ono L.K., Qi Y. Lithium-ion batteries: outlook on present, future, and hybridized technologies. *Journal of Materials Chemistry A*. 2019; 7(7): 2942. https://doi.org/10.1039/c8ta10513h
13. Deng X., Li J., Ma L., J. Sha, Zhao N. Three-dimensional porous carbon materials and their composites as electrodes for electrochemical energy storage systems. *Materials Chemistry Frontiers*. 2019; (11): 2221–2245. https://doi.org/10.1039/C9QM00425D
14. Kim T., Song W., So Y., Qi Y. Linium-ion batteries: outloo and hybridized technologies. *Journal of Materials Chemistry A*. 2019; 7(7): 292. https://doi.org/10.1039/D3TA01384G
15. Chernysheva M.N., Rychagov A.Yu., Kornilov D.Yu., Tkachev S.V., Gubin S.P. Investigation of sulfuric acid intercalation into thermally expanded graphite in order to optimize the synthesis of electrochemical graphene oxide. *Journal of Electroanalytical Chemistry*. 2020; 858: 113774. https://doi.org/10.1016/j.jelechem.2019.113774
16. Shang W., Yu W., Tan P., Chen B., Wu Zh., Xud H., Ni M. Achieving high energy density and efficiency through integration: progress in hybrid zinc batteries. *Journal of Materials Chemistry A*. 2019; 7(26): 15564. https://doi.org/10.1039/C9TA04710G
17. Koz'menkova A.Ya. Positive electrodes of lithium-oxygen batteries based on binary titanium compounds. Diss. Cand. Sci. (Eng.). Moscow; 2018. 147 p. (In Russ.)
18. Gorokhovsky A.V., Palagin A.I., Panova L.G., Ustinova T.P., Burmistrov I.N., Aristov D.V. Manufacturing submicro-nanoscale potassium polytitanates and composite materials based on them. *Nanotekhnika = Nanotechnics*. 2009; (3): 38–44. (In Russ.)
19. Sanchez-Monjaras T., Gorokhovsky A.V., Escalante-Garcia J.I. Molten salt synthesis and characterization of polytitanate ceramic precursors with varied TiO_2/K_2O molar ratio. *Journal of the American Ceramic Society*. 2008; 91(9): 3058–3065. https://doi.org/10.1111/j.1551-2916.2008.02574.x
20. Miller J.R., Simon P. Materials science: electrochemical capacitors for energy management. *Science*. 2008; 321(5889): 651–652. https://doi.org/10.1126/science.1158736
21. Chen X., Paul R., Dai L. Carbon-based supercapacitors for efficient energy storage. *National Science Review*. 2017; 4(3): 453–489. https://doi.org/10.1093/nsr/nwx009
22. Choi J.U., Voronina N., Sun Y.-K., Myung S.-T. Recent progress and perspective of advanced high-energy co-less Ni-rich cathodes for Li-ion batteries: Yesterday, today, and tomorrow. *Advanced Energy Materials*. 2020; 10(42): 2002027. https://doi.org/10.1002/aenm.202002027
23. Wen P., Gong P., Sun J., Wang J., Yang S. Design and synthesis of Ni-MOF/CNT composites and rGO/carbon nitride composites for an asymmetric supercapacitor with high energy and power density. *Journal of Materials Chemistry A*. 2015; 3(26): 13874. https://doi.org/10.1039/C5TA02461G
24. Xu J., Yang C., Xue Y., Wang C., Cao J., Chen Z. Facile synthesis of novel metal-organic nickel hydroxide nanorods for high performance supercapacitor. *Electrochimica Acta*. 2016; 211: 595–602. https://doi.org/10.1016/j.electacta.2016.06.090
25. Wu J., Wei F., Sui Y., Qi J., Zhang X. Interconnected NiS-nanosheets@porous carbon derived from Zeolitic-imidazolate frameworks (ZIFs) as electrode materials for high-performance hybrid supercapacitors. *International Journal of Hydrogen Energy*. 2020; 45(38): 19237–19245. https://doi.org/10.1016/j.ijhydene.2020.05.061
26. Ji F., Jiang D., Chen X., Pan X., Kuang L., Zhang Y., Alameh K., Ding B. Simple in-situ growth of layered Ni_3S_2 thin film electrode for the development of high-performance supercapacitors. *Applied*

Surface Science. 2017; 399: 432–439. https://doi.org/10.1016/j.apsusc.2016.12.106

27. Javed M.S., Aslam M.K., Asim S., Batool S., Idrees M., Hussain Sh., Shah S.Sh.Ah., Saleem M., Mai W., Hu Ch. High-performance flexible hybrid-supercapacitor enabled by pairing binder-free ultrathin Ni–Co–O nanosheets and metal-organic framework derived N-doped carbon nanosheets. *Electrochimica Acta.* 2020; 349: 136384. https://doi.org/10.1016/j.electacta.2020.136384
28. Zheng L., Song J., Ye X., Wang Y., Shi X., Zheng H. Construction of self-supported hierarchical NiCo-S nanosheet arrays for supercapacitors with ultrahigh specific capacitance. *Nanoscale.* 2020; 12(25): 13811–13821. https://doi.org/10.1039/d0nr02976a
29. Sleptsov V.V., Kukushkin D.Yu., Kulikov S.N., Diteleva A.O. Thinfilm nanotechnologies for creating power supply sources. *Vestnik mashinostroeniya*. 2021; (2): 65–67. (In Russ.). https://doi.org/10.36652/0042-4633-2021-2-65-67
30. Sleptsov V.V., Kozhitov L.V., Muratov D.G., Popkova A.V., Savkin A.V., Diteleva A.O., Kozlov A.P. Thin film vacuum technologies for a production of highly capacitive electrolytic capacitors. *Journal of Physics Conference Series. Materials of 26th Inter. conf. on Vacuum Technique and Technology. June 18–20, 2019, St. Petersburg, Russian Federation.* 2019; 1313: 012051. https://doi.org/10.1088/1742-6596/1313/1/012051
31. Goffman V.G., Sleptsov V.V., Gorokhovsky A.V., Gorshkov N.V., Kovyneva N.N., Sevryugin A.V., Vikulova M.A., Bainyashev A.M., Makarova A.D., Zaw Lwin K. Energy storage with titanium modified busopytic electrodes. *Elektrokhimicheska Energetica*. 2020; 20(1): 20–32. (In Russ.). https://doi.org/10.18500/1608-4039-2020-20-1-20-32
32. Elinson V.M., Shchur P. Study of the surface of antimicrobial barrier layers based on fluorocarbon and carbon films. In: *Astashynski V.M., Gusarov A.V., Cherenda N.N., eds. High Temperature Material Processes: An International Quarterly of High-Technology Plasma Processes.* 2022; 4(26): 11–26. https://doi.org/10.1615/HighTempMatProc.2022043894
33. Sleptsov V., Diteleva A. Thin-film technology for creating flexible supercapacitor electrodes based on a carbon matrix. *High Temperature Material Processes.* 2020; 24(3): 167–171. https://doi.org/1010.1615/HighTempMatProc.2020035840